Cross-correlation trajectory study of V-V energy transfer in HF-HF and DF-DF^{a)}

M. E. Coltrin

Department of Chemistry, University of Illinois, Urbana, Illinois 61801 and Sandia National Laboratories, Albuquerque, New Mexico 87185

M. L. Koszykowski

Sandia National Laboratories, Livermore. California 94550

R. A. Marcus

A. A. Noyes Laboratory of Chemical Physics, California Institute of Technology, Pasadena, California 91125 (Received 13 March 1980; accepted 11 July 1980)

Results of a fully three-dimensional classical trajectory calculation of vibrational energy transfer are presented for the collision of HF(v=1) with HF(v=1) and its deuterium analog. A cross-correlation method, together with quasiclassical trajectories, is introduced to relate the changes in vibrational states of the two molecules to probabilities and rate constants. Multiple collisions are found to make an important contribution to the vibrational energy transfer cross-sections for the present potential surface. Vibrational anharmonicity is shown to decrease the energy transfer rate constant by a factor of ten, by causing the process to be further from exact resonance. Excellent agreement with experiment is obtained for the HF-HF and DF-DF systems.

I. INTRODUCTION

In this paper a quasiclassical trajectory study of the very efficient vibration-to-vibration (V-V) collisional energy transfer for hydrogen fluoride (HF-HF) and deuterium fluoride (DF-DF) is presented. The calculation is fully three dimensional, i.e., with each molecule having three translational, two rotational, and one vibrational degrees of freedom. A cross-correlation method is used to extract state-to-state cross sections and rate constants.

For the past decade or two, there has been increasing use of the quasiclassical trajectory approach for calculating properties of molecular collisions. The classical trajectory method has been reviewed in detail^{1,2} and is the subject of much current interest.³ Quasiclassical trajectories are used in many circumstances where a quantum mechanical approach would be prohibitively lengthy and therefore costly.

There have been a few "exact" numerical quantum mechanical calculations of vibration-vibration energy transfer, 4-7 all thus far limited to the collinear geometry because of the very large number of open channels that must be included when the molecules are allowed to rotate. Several excellent review articles on the development of vibrational energy transfer calculations are available. Beven for the classical trajectory approach, only a limited number of studies of vibration-vibration energy transfer in systems involving four or more atoms have been attempted for other than a collinear geometry. The studies of diatom-diatom collisions. 14,15

b)Present address.

Bass and Thompson¹⁴ studied the vibrational relaxation of Cl_2 by HCl and DCl over the temperature range 800-2100 K and the self-relaxation of HCl over the temperature range 1600-2600 K. Their calculation is a fully three-dimensional quasiclassical study employing a semiempirical valence-bond potential energy surface. They were interested in vibrational relaxation due to the V-R, T mechanism and did not try to extract V-V rate constants.

Wilkins¹⁵ in his recently published classical trajectory study of mechanisms of vibrational deactivation in HF calculates both the V-V and V-R, T rates. In later sections of the present paper we discuss the similarities and differences between our calculations and those of Wilkins. ¹⁵

There has also been recent work on vibrational relaxation in the HF-HF system using a "classical path" approach. 19-21 This approach involves treating the translational and rotational degrees of freedom classically (by performing rigid-rotor trajectories). The vibrational degrees of freedom are then treated quantum mechanically by solving the time-dependent "forced oscillator" Schrödinger equation: The intermolecular potential experienced by the vibrations of each HF molecule during the trajectories (of rigid rotors) is used as a time-dependent perturbation on the vibrating molecules. A comparison with these previous results is given later.

The rate of vibrational deactivation of HF has been the subject of considerable experimental study, ²²⁻²⁴ due to its relevance to the performance of HF chemical lasers. In an HF chemical laser, vibrationally excited HF molecules can be produced by the highly exothermic reactions²²⁻²⁴

$$F + H_2 - H + HF^*$$
 (1.1)

a)This work supported by the U.S. Department of Energy.

$$H + F_2 - F + HF^*$$
 (1.2)

For Reaction (1.1) there is enough energy to populate vibrational states up to level three, with level two being experimentally the most probable. Reaction (1.2) is observed to populate HF vibrational levels up to nine, with five and six being most probable. The distribution of product HF vibrational states is, of course, a nonthermal distribution and the resultant population inversion gives rise to the lasing process. The main source of power loss of the HF laser is due to collisional deactivation of the upper vibrational levels. For this reason there has been much recent interest in the experimental and theoretical study of the rates of these collisional relaxation processes. The experimental work on HF relaxation is described in Refs. 15 and 22-24.

In the present paper, V-V energy transfer is studied for the reaction

$$HF(v=1) + HF(v=1) - HF(v=2) + HF(v=0)$$
 (1.3)

and for its deuterium analog. The V-V cross sections and rate constants are calculated using quasiclassical trajectories and a cross-correlation method of analysis. In this analysis method, correlations in the changes in vibrational state of the two molecules are related to quantum mechanical probabilities. The method is similar in spirit to the moment method of analysis. 25,26 A justification for relating quasiclassical averages to quantum mechanical probabilities has been given 27 using semiclassical arguments.

In Sec. II the intermolecular potential in the HF-HF system is discussed. Section III gives a few details for the quasiclassical trajectories and the method used here for calculating vibrational action-angle variables is described. The cross-correlation method of analysis employed in the present work is presented in Sec. IV, the results of our calculations of V-V energy transfer are given in Sec. V, and a summary is given in Sec. VI. The Appendix gives details of one of the two potential energy surfaces employed here.

II. INTERMOLECULAR POTENTIAL FOR THE HF-HF SYSTEM

Except where otherwise stated, the potential energy surface we have used is an analytical fit by Poulsen et al. ¹⁹ to an ab initio SCF surface of Yarkony et al. ²⁸ plus a correction ¹⁹ for dispersion terms. The fit is based on atom-atom interactions plus the dipole-dipole term. (An alternative fit ²⁹ to the SCF surface based on an expansion in Legendre polynomials with no vibrational dependence of the short range repulsions is less suitable for our purposes, for integrating the classical equations of motion.) The dispersion term was taken ¹⁹ as $-C_6/R^6$ with $C_6 = 46.5 \times 10^{-60}$ erg cm⁶.

We also investigated an alternative, more approximate, surface based on a Stockmayer potential. 30 We used the surface of Ref. 31 for a pair of rigid rotors, but with a dependence of the dipole-dipole term on vibrational distances. 32 The details of the surface, including the method of obtaining the parameters, are given in the Appendix.

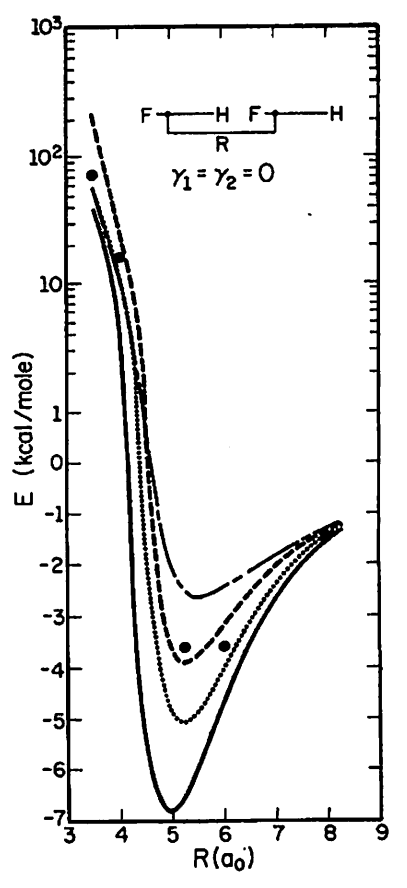


FIG. 1. Comparison of SCF ab initio points of Yarkony et al. 28 (large dots), the fit of Poulsen et al. 19 to SCF data (curve of small dots), the curve of Poulsen et al. 19 with addition of the spherically symmetric dispersion term (solid curve), the Stockmeyer potential (dashed curve), and the potential of Wilkins 15 (long dashshort dashed curve). The molecules are in the attractive collinear arrangement with dipoles parallel. Equation (A. 2) describes the angles of orientation.

One notable difference between these two surfaces is in the depth of the well in the attractive configuration (6.9 kcal mol⁻¹ in Ref. 19 vs 3.9 kcal mol⁻¹ in the Appendix). Thus, the surface in Ref. 19 is expected to give more trajectories forming quasibound intermediates than the surface in the Appendix, an expectation which is confirmed by results given later.

We conclude this section with a description of the potential energy surface of Wilkins. Wilkins has used an atom-atom LEPS (London-Eyring-Polanyi-Sato) potential energy surface to describe the short-range interactions in HF-HF. The atom-atom LEPS parameters are those derived from previous work on three-body interactions involving hydrogen and fluorine atoms. The long-range Coulombic interactions are described by placing a fractional point charge on each atom. Plots of cuts of each potential energy surface discussed here are given in Figs. 1-4. The orientation angles γ_1 , γ_2 , and ψ are described by Eq. (A2). A distinctive feature seen in Fig. 1 is the shallowness of the attractive well predicted by the surface in Ref. 15 (2.7 kcal mol⁻¹).

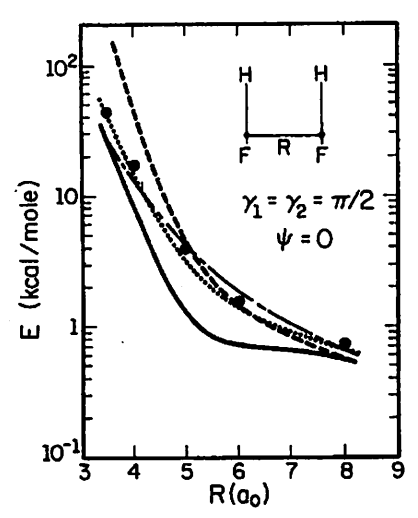


FIG. 2. Same as Fig. 1, but with the orientation $\gamma_1 = \gamma_2 = \pi/2$, $\psi = 0$.

III. SELECTION OF INITIAL CONDITIONS AND QUASICLASSICAL TRAJECTORIES

The initial conditions for our quasiclassical trajectories were chosen using the Monte Carlo technique. ³³ The rotational angular momentum of each molecule and the initial relative velocity are chosen at random from the appropriate Maxwell-Boltzmann distributions at a given temperature. ³⁴⁻³⁶ The "angle" variables that are conjugate to the classical "action" variables and which specify relative orientations, rotational phases, and

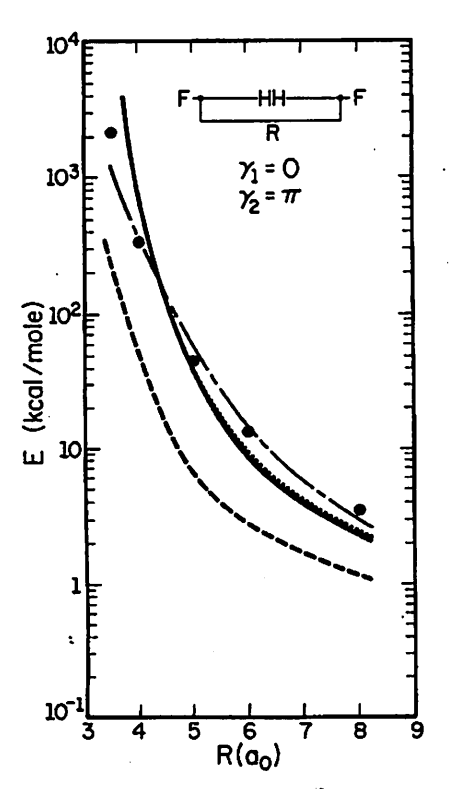


FIG. 3. Same as Fig. 1, but with the orientation $\gamma_1 = 0$, $\gamma_2 = \pi$.

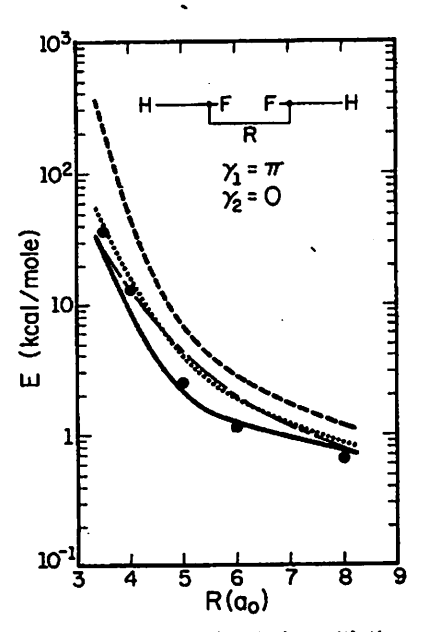


FIG. 4. Same as Fig. 1, but with the orientation $\gamma_1 = \pi$, $\gamma_2 = 0$.

vibrational phases are chosen as random numbers from uniform distributions lying between 0 and $1.^{36}$ The method used here for selection of all initial conditions, with the exception of those associated with the vibrations and the impact parameter, is the same as that explained in detail elsewhere. $^{34-36}$

The problem of assigning action-angle variables for the vibrational motion merits further consideration. Porter, Raff, and Miller have considered the problem of a rotating-vibrating Morse oscillator. 37 Because of the coupling between the rotation and vibration, one cannot obtain an analytical solution for the vibrational action-angle variables. Porter et al. 37 expanded the r^{-2} term that appears in the classical Hamiltonian in a Taylor's series about $r=r_e$, where r_e is the equilibrium internuclear separation. By truncating their expansion after three terms, they obtained expressions that could be solved analytically for the action-angle variables. Expressions were then obtained for calculating the vibrational action, angle, turning points, and radial probability density function. These expressions were easy to evaluate and use. Of course, because they are based on a truncated expansion, the formulas obtained are only approximate and caution is needed in their use. The approximation becomes better the smaller the amplitude $r-r_e$. In using the method of Porter et al. 31 care is needed in selecting the initial conditions such that $r \approx r_e$. (To obtain the proper distribution of oscillator separations one appropriately adjusts R, the initial intermolecular separation.) Also, as noted in Ref. 37, the approximation becomes worse as the rotational energy becomes greater, due to increased centrifugal distortion. While the method of Ref. 37 is very useful for the system where a lesser degree of accuracy in handling the vibrations can be tolerated, for many systems the average amount of vibrational energy change due to collisions is as small as the error incurred by the truncation. (An example of a small probability is that of collisional deactivation of vibrationally excited

TABLE I. Comparison of methods for calculating vibrational quantum numbers for typical final trajectory conditions.

Energy ^a	J ^b	Numerically exact ^c	Porter, Raff and Miller ^d	Muckerman ^e
0.814839	4,2495	1, 054285	1.054228	1,054691
0. 658043	0.9074	0.816340	0.816338	0,816167
0.746866	4.0464	0, 920850	0.920806	0.921155
0.874404	2,4536	1,241653	1.241631	1.241644
0.651257	0.7156	0.803911	0.803910	0.803730
0.779958	5.0707	0.941917	0.941843	0.942517
0.781826	1.8702	1.060071	1.060061	1.059965
0.536309	0.8729	0.566367	0.566366	0.566225
0.751015	2, 2275	0.988167	0.988153	0.988113
0.533887	2.2871	0.538544	0.538538	0, 583505

^{*}Total internal energy of the molecule in eV.

HCl by ground state HCl, found experimentally to be 38 1.27×10⁻⁴.) The numerical procedure involves an iterative solution of the usual semiclassical quantization condition for a vibrational motion. No approximation involving neglect of vibration-rotation coupling was made (either here or in Ref. 37).

In Table I we present a comparison of typical trajectory results for the final vibrational quantum number using the numerical method used here (column 3) and the approximate method of Ref. 37 (column 4). It is readily seen that the approximate method gives good results, typically affording at least four figures of accuracy. For the HF-HF system, where transition probabilities are rather large, this degree of accuracy is sufficient. Also, for other applications of classical trajectories such as three-body reactive scattering calculations where final vibrational states can be distributed over a wide range, the approximate formulas of Ref. 37 provide quite adequate accuracy and are easier to use than the numerical method. However, in making our four-body trajectory program as general as possible, we have used the more accurate numerical evaluation of the vibrational action-angle variables to enable us to study other systems where changes in vibrational quantum number are very small. 38 The added computational time in the numerical method is negligible.

Another, more approximate method of calculating the initial and final vibrational quantum numbers has been given by Muckerman [Ref. 39, Eqs. (5a)-(5g)]. In Table I we compare typical vibrational quantum numbers calculated using the method of Ref. 39 (column 5) and the other two methods described above.

Analysis of the results of the three methods illustrated in Table I shows that the root mean squared (rms) deviation of the method of Porter et~al. ³⁷ from the numerically exact method of this Appendix is 5×10^{-5} , while the rms deviation of the more approximate formulas ³⁹ is 4×10^{-4} . Thus, the method of Ref. 37 typically yields four to five digits of accuracy and the method of Ref. 39 about one digit less. Keeping these figures in mind, one can choose the method of analyzing the vibrational quantum numbers according to the degree of accuracy needed.

The impact parameter was selected by Monte Carlo sampling using a stratified sampling technique. ^{33,40} In this stratified sampling technique, one samples more extensively from the impact parameters which contribute most to the inelastic cross section for energy exchange. ⁴¹ One also can do the sampling by another technique (importance sampling ³³) as in Ref. 42. In general, it was necessary in the present case to consider impact parameters of 6 to 8 Å before contributions to the inelastic cross section became negligible.

The initial separation between the centers of mass of the two molecules (R) was 10 Å for each trajectory. This R was large enough to ensure a negligible interaction at the beginning of each trajectory $(-0.1k_BT)$.

After the initial conditions for a trajectory were selected in the above coordinates, they were converted to nine Cartesian coordinates and their nine conjugate momenta, ³⁶ namely, to the three relative coordinates for each molecule and three relative coordinates for the separation of the centers of mass of the two molecules. The classical trajectory was computed by numerically integrating the 18 Hamilton equations of motion. For the integration of the collision trajectory and the integration required in evaluating the vibrational action-angle variables the subroutine DEROOT⁴³ was used. The trajectory was integrated until the final separation of collision partners was again 10 Å.

The trajectory calculations were performed on a CDC-175 computer. On the average, each trajectory required 45 s computation time.

IV. CALCULATION OF FINAL STATES, CROSS SECTIONS, AND RATE CONSTANTS

A. Method for determining final vibrational states

The final rotational angular momentum and energy of each molecule and relative velocity of the collision partners are readily calculated from the final Cartesian coordinates of the trajectory. The final action-angle variables can be obtained via the transformations in Ref. 36 for all of the degrees of freedom except the vibrations, and the latter are treated as follows:

The final classical vibrational quantum number is, in general, not an integer. From each molecule's final total energy and angular momentum, its final vibrational state can be calculated by a numerical integration over one cycle of the motion (i.e., the usual semiclassical specification of vibrational state).

B. Cross-correlation method for the HF(v=1) + HF(v=1) system

In calculating the rate constants for vibrational energy transfer we introduce a cross-correlation method of analysis. We then assume that the quasiclassical and quantum mechanical moments, ^{25,28} and the cross correlations of the distribution of final averages of internal energies, quantum numbers, etc., are equal. We then relate the correlation in changes of vibrational state of each molecule to probabilities and rate constants.

One can formally write an expression for the quantum

Reference 37.

^{*}Reference 39.

mechanical expectation value of the following cross correlation between the change in vibrational state of molecules 1 and 2 for a given value of the orbital angular momentum and the relative velocity:

$$(\Delta v_1, \Delta v_2)_{QM} = P_{20,11}(+1)(-1) + P_{02,11}(-1)(+1) + P_{01,11}(-1)(0) + P_{10,11}(0)(-1),$$
 (4.1)
= $-P_{20,11} - P_{02,11} = -P_{V-V},$ (4.2)

where $P_{kl,ij}$ is the probability for the vibrational transitions i-k and j-l of molecules 1 and 2, respectively. Both terms $P_{20,11}$ and $P_{02,11}$ contribute to V-V vibrational change of molecule 1, the probability of which is denoted P_{V-V} . Multiquantum transitions have been neglected in writing Eq. (4.1).

The probability for V-R, T suffered by molecule 1 is $P_{01,11}$. To obtain it we consider

 $\langle \Delta v_1 . (\Delta v_1 + \Delta v_2) \rangle_{QH}$

$$= P_{20,11}(+1)(+1-1) + P_{02,11}(-1)(+1-1) + P_{01,11}(-1)(-1+0) + P_{10,11}(0)(0-1),$$
 (4.3)

$$=P_{01,11}=P_{V-R,T}. (4.4)$$

The advantage of considering the cross correlations such as in Eqs. (4.2) and (4.4) is that one obtains directly the quantities of interest P_{V-V} and $P_{V-R,T}$. Another way of obtaining P_{V-V} and $P_{V-R,T}$ is from the first and second moments of Δv_1 . However, this method yields linear combinations of P_{V-V} and $P_{V-R,T}$ and their values must be obtained by additions and subtractions of the two moments. This was found to lead to large standard errors, particularly for the small quantity $P_{V-R,T}$, where use of the first and second moments gave a standard error ten times larger than obtained via the cross correlations.

The above probabilities depend on the impact parameter b via a dependence on the orbital angular momentum and on the initial relative velocity V_R .

On making the assumption that the quantum mechanical expectation values equal those determined from a quasiclassical trajectory calculation, ^{25,27} one obtains

$$P_{V-V}(b, V_R) = -\langle \Delta v_1, \Delta v_2 \rangle_{qa}(b, V_R)$$
 (4.5)

and

$$P_{V-R,T}(b, V_R) = \langle \Delta v_1 \cdot (\Delta v_1 + \Delta v_2) \rangle_{qq}(b, V_R), \qquad (4.6)$$

where the subscript qa denotes "quasiclassical average." The b and V_R above indicate that these probabilities are for a given impact parameter and relative velocity, respectively.

The theoretical V-V cross section is found by integrating over impact parameters

$$\sigma_{V-V}(V_R) = 2\pi \int_0^\infty P_{V-V}(b, V_R)b \, db$$
 (4.7)

The impact parameter integral is evaluated using the Monte Carlo stratified sampling technique. 33,40,41 The theoretical V-V rate constant is related to the cross section as

$$k_{V-V}(T) = \langle V_R \sigma_{V-V}(V_R) \rangle \langle T \rangle . \tag{4.8}$$

The average in Eq. (4.8) is over a Maxwell-Boltzmann distribution of relative velocities at temperature T. Expressions analogous to Eqs. (4.7) and (4.8) are used to calculate the V-R, T cross section and rate constant, respectively.

Experimentally, the observed rate of formation of HF(v=2) in Reaction (1.3) is determined and related to the observed V-V rate constant

$$d[HF(v=2)]/dt = k_{v-v}^{OBS}[HF(v=1)]^2$$
, (4.9)

$$= \frac{1}{2}k_{v-v}[HF(v=1)]^2, \qquad (4.10)$$

where k_{V-V} would be the rate constant if the molecules were distinguishable. It is given by Eq. (4.8). The factor of $\frac{1}{2}$ used to relate the rate constants of Eqs. (4.8) and (4.9) is necessary to account for the indistinguishability of the two molecules.

V. RESULTS

A. HF(v=1) + HF(v=1) system using Morse vibrational potentials

In this section the results of our quasiclassical trajectory investigation of vibrational energy transfer are presented for the collision (1.3) at 300 K, using the intermolecular potential of Ref. 19. For the intramolecular vibrational potential energy of each molecule a Morse potential was used, the parameters for which were determined from spectroscopic constants. (In Ref. 19 a harmonic oscillator potential was used instead.)

Using the method of selecting initial conditions and of calculating final results described earlier, the rate constant for V-V energy transfer for HF-HF as given in Eq. (1.3) is calculated to be 9.0×10^{12} cc mol⁻¹ s⁻¹. The standard error in this rate constant is 1.2×10^{12} cc mol⁻¹ s⁻¹.

The V-R, T rate constant for this set of collision partners is 4.8×10^{10} cc mol⁻¹ s⁻¹, with standard error of 7.2×10^{10} cc mol⁻¹ s⁻¹. Although the standard error for the V-RT rate constant is large, it appears that the V-R, T process is at least 100 times slower than the V-V.

The theoretical V-V rate constant can be compared with an experimental one determined by Cohen and Bott⁴⁴ using a laser-induced fluorescence technique. They found the value to be 10.5×10^{12} cc mol⁻¹ s⁻¹ at 300 K, while our theoretical rate constant is 9×10^{12} cc mol⁻¹ s⁻¹. The agreement is remarkably close, noting that no adjustable parameters have been used.

B. Correlation coefficients of energy disposal

To illustrate further that in the present study the V-V energy transfer really dominates the collision, we look at the correlation coefficient for the change in vibrational state of one molecule and the change in the other. An estimate of the population correlation coefficient between two variables, say x and y, is given by

$$r = \left[\sum_{i} (x_i - \overline{x})(y_i - \overline{y}) \right] / \left[\sum_{i} (x_i - \overline{x})^2 \right] \left[\sum_{i} (y_i - \overline{y})^2 \right].$$
(5. 1)

TABLE II. Correlation coefficient for changes in dynamic variables for the $HF(v_1=1)+HF(v_2=1)$ system.^a

x	у	Correlation coefficient ^b
Δv_1	Δv_2	-0.9957
Δv_1	$\Delta(J_1)$	0.0197
Δv_1	$\Delta(J_1^2)$	0.0601
Δv_1	ΔJ_2	-0.0059
Δv_1	$\Delta (J_2^2)$	-0.0160
ΔJ_1	ΔJ_2	- 0, 4248
$\Delta(J_1^2)$	$\Delta(J_2^2)$	-0.4722
ΔE trans	$\Delta(J_1^2+J_2^2)$	-0.9317

^aPotential energy surface from Ref. 19, Morse vibrational potential, 300 K.

By application of Schwarz's inequality one can determine that $-1 \le r \le 1$. If r=1, then x and y show a perfect, positive linear correlation; if r=-1, x and y have a perfect, negative linear correlation; and if r=0, there is no linear correlation between x and y.

In Table II the correlation coefficient is given for transfer of vibrational quanta (really, of classical action v) from one molecule to the other. For a pure V-Vprocess, r for correlation between Δv_1 and Δv_2 would be -1. From Table II one sees that our trajectory data yield r = -0.9957 for the V-V process. From the data in Table II one can also look for evidence of V-R, T energy transfer in this system. One sees that there is essentially no linear correlation between the change in vibrational quantum number (v_i) , the vibrational action variable) of one molecule and the change in the rotational quantum number $(J_1, rotational action variable)$ of the same molecule, or in the change in approximate rotational energy of the same molecule (proportional to J_1^2), or in the change in rotational quantum number (U_2) of the other molecule, or in the change in approximate rotational energy of the other molecule (proportional to J_2^2). Thus, one concludes that for this HF(1) + HF(1) system. neither intermolecular nor collision-induced intramolecular vibration-to-rotation energy transfer are important. There is, however, an appreciable correlation between the change in rotational quantum number of one molecule and the change of rotational quantum number of the other $(\Delta J_1 \text{ vs } \Delta J_2)$, reflecting some tendency to a statistical distribution among the R and T coordinates. A similar correlation is seen in the "rotational energy" changes of each molecule $[\Delta(J_1^2)$ vs $\Delta(J_2^2)]$. Finally, the change in total rotational energy (proportional to $J_1^2 + J_2^2$) is seen to have a strong linear, negative correlation with the change in translational energy (E_{trans}) of relative motion, a result which also follows from the $\Delta v_1 - \Delta v_2$ correla-

In summary, using the potential energy surface of Poulsen et al., 19 our theoretical V-V rate constant is

found to agree closely with the experimental value. The vibrational relaxation for an individual molecule occurs almost exclusively via the V-V mechanism. The rotational relaxation is primarily due to a R-R, T process.

As discussed in Sec. II of this paper, this potential energy surface for the HF-HF system has an attractive well of approximately 6.9 kcal mol⁻¹. One would predict the formation of long-lived, quasibound complexes, i.e., trajectories in which orbiting occurs. In our trajectory program we recorded the number of times that the product $\mathbf{R} \cdot (d\mathbf{R}/dt)$ changes sign. For a simple collision, where the two molecules approach, reach some minimum distance, and then separate, this function changes sign once. If N_{sign} is the number of times that $\mathbf{R} \cdot (d\mathbf{R}/dt)$ changes sign for a given trajectory, then $(N_{\text{sign}}-1)/2$ is taken to be the number of repeated encounters for that trajectory. We shall call this encounter a multiple collision.

We find that for the system studied here multiple collisions occur in 30% of the trajectories. However, the trajectories that have multiple collisions accounted for 60% of the V-V rate constant. The trajectories that exhibit these multiple collisions are thereby computed to be about a factor of 3.5 more efficient in transferring vibrational energy. [The relative efficiency of the multiple collision trajectories is $(0.6/0.3)\times(1-0.3)/(1-0.6)$, i.e., 3.5.] This behavior is not surprising: Each encounter in the multiple collision is able to contribute to vibrational energy transfer. The average number of encounters within a multiple collision was five, but sometimes was as great as 100.

C. HF(V=1) + HF(V=1) system using harmonic oscillator vibrational potentials

In the preceding calculation a Morse oscillator potential was used for the vibrational potential of each molecule. However, harmonic oscillator potentials are frequently used in collision problems. To investigate the effect of the anharmonicity on the above V-V rate constant a comparison with harmonic oscillator results is given. In the absence of rotations, the V-V process of Reaction (1.3) is exactly resonant for the case of a harmonic potential but not for a Morse potential, i.e., the total vibrational energy of the reactants equals that of the products in the harmonic case. For the Morse oscillator potential there is an energy mismatch and the process is off resonance due to this vibrational anharmonicity.

On repeating the above calculation for Reaction (1.3) but using a harmonic oscillator vibrational potential (obtained from the quadratic term of a series expansion of the Morse potential), the V-V rate constant was calculated to be 9.4×10^{13} cc mol⁻¹ s⁻¹ (standard error 1.2 $\times10^{13}$ cc mol⁻¹ s⁻¹). This rate constant can be compared with 9.0×10^{12} cc mol⁻¹ s⁻¹, the rate constant calculated for the Morse oscillator case. Thus, classical resonance of the V-V process has yielded a rate constant 10 times higher for the harmonic oscillator case over the anharmonic one.

In the harmonic oscillator case the V-R, T rate constant was again found to be negligibly small.

^bSee Eq. (5.1).

D. HF(v=1) + HF(v=1) system using the Stockmayer intermolecular potential

Following the same procedure as before, but using the Stockmayer potential described in the Appendix, the rate constant for V-V energy transfer was calculated to be 2.1×10^{12} cc mol⁻¹ s⁻¹ (standard error 3×10^{11} cc mol⁻¹ s⁻¹). This rate constant is compared with the value of 9.0×10^{12} cc mol⁻² s⁻¹ calculated above using the surface in Sec. II. ¹⁹

We have noted earlier that the difference in the two calculations is in the form of the intermolecular potential, such that the well depth was substantially smaller (3.9 vs 6.9 kcal mol⁻¹) for the surface in the Appendix. One would thus expect fewer multiple-collision trajectories in the case of the Stockmayer potential, an expectation confirmed by the present calculations: Multiple collisions were found to occur in only 9% of the trajectories using the modified Stockmayer potential, compared to 30% in the case of the surface in Sec. II. ¹⁹ As noted earlier, the multiple collisions contributed very significantly to the V-V cross section for the surface in Sec. II.

One reason for the rate constant obtained with the Stockmayer potential being a factor of 4 times less than the one calculated using the surface in Sec. II is the sparsity of multiple collisions. However, the difference in multiple collisions (associated with the attractive portion of the intermolecular potential) does not account for all of the factor of 4. We calculated the contribution to the V-V rate constant of the trajectories that are not multiple-collision type to be 1.9 $\times 10^{12}$ and 3.6 $\times 10^{12}$ cc mol-1 s-1 for the modified Stockmayer and Sec. II surfaces, respectively. (Recall that the rate constants including all trajectories were 2.1×10^{12} and 9.0×10^{12} cc mol-1 s-1, respectively.) The fact that even when the multiple-collision trajectories are excluded the V-Vrate constant is still roughly a factor of 2 smaller for the Stockmayer case may be due to differences in the short-range repulsive terms in the potentials: The short-range repulsive part of the Sec. II surface depended on the vibrational coordinates while that based on the simpler Stockmayer did not, and so only the former could contribute to vibrational energy transfer.

E. DF(v=1) + DF(v=1) system

We have also studied vibration-to-vibration energy transfer for the reaction

$$DF(v=1) + DF(v=1) - DF(v=2) + DF(v=0)$$
 (5. 2)

at 300 K. The intermolecular potential in Sec. II¹⁹ was used, but with the Morse oscillator intramolecular vibrational potential determined from spectroscopic measurements⁴⁵ as before. The same methods as for the HF-HF case were used for sampling initial conditions, integrating trajectories, and determining cross sections and rate constants. For the DF-DF reaction in Reaction (5.2) the V-V rate constant was calculated to be 1.7×10^{13} cc mol⁻¹ s⁻¹ (standard error 2.5×10^{12} cc mol⁻¹ s⁻¹). This result compares well with the experimental value of Bott⁴⁶ 1.9×10^{13} cc mol⁻¹ s⁻¹ at 295 K.

As one would expect, the dynamics of the V-V trans-

TABLE III. Correlation coefficient for changes in dynamical variables for the DF($v_1 = 1$) + DF($v_2 = 1$) system. ^a

		Correlation
x	y .	· coefficient ^b
Δv_1	Δv_2	-0.9981
Δv_1	ΔJ_1	-0.0643
Δv_1	$\Delta(J_1^2)$	-0.0895
Δv_1	ΔJ_2	0.0592
Δv_1	$\Delta(U_2^2)$	0,0295
ΔJ_1	ΔJ_2	-0.5822
$\Delta(J_1^2)$	$\Delta(J_2^2)$	-0.6289
ΔE trans	$\Delta(\boldsymbol{J}_1^2 + \boldsymbol{J}_2^2)$	- 0. 9525

^aPotential energy surface from Ref. 19, Morse vibrational potential, 300 K.

fer in DF-DF are very similar to that in the HF-HF case. Again, multiple collisions contributed substantially to the V-V rate constant. Multiple collisions were observed in 37% of the trajectories and accounted for 70% of the V-V rate constant.

In Table III the calculated correlation coefficients are listed for changes in dynamical variables in the DF-DF system. These correlation coefficients are seen to be very similar to those calculated for the HF-HF case (Table II). There is again a strong negative correlation between the change in vibrational state of one molecule and the change in vibrational state of the other. As in the HF-HF system, there is no evidence for either a collision-induced intramolecular or an intermolecular vibration-to-rotation energy transfer mechanism under these conditions.

F. Comparisons with other work

Some of the findings in this section can be compared to those of Wilkins, ¹⁵ who studied vibrational relaxation in HF systems using the quasiclassical trajectory approach.

The present calculations differ in many aspects from those of Ref. 15, e.g., in the potential energy surface used. A major difference between the LEPS surface¹⁵ and that of Sec. II¹⁹ lies in the well depth of 2.7 kcal mol⁻¹ compared to 6.9 kcal mol⁻¹. It is not surprising that Wilkins' trajectory study indicates that multiple collisions do not occur for the typical HF-HF collisions at 300 K, ¹⁵ in contrast to our findings using the potential energy surface in Sec. II. ¹⁹

Other differences were in the initial conditions for the trajectories, namely, in the initial separation of the centers of mass of the two molecules (8 Å in Ref. 15 vs 10 Å here) and in the maximum impact parameter considered (2.5 Å vs 6-8 Å here). Another difference was in the method of determining the V-V probability from the trajectory data. We have used the cross-correlation

See Eq. (5. 1).

TABLE IV. Comparison of calculated V-V rate constants using Methods I and II.

	Rate constant (10 ¹³ cc mol ⁻¹ s ⁻¹	
System	Method I	Method II
HF-HF-Morse oscillators	0,9	6, 2
HF-HF-Harmonic oscillators	9.4	23.0
HF-HF-Stockmayer potential	0, 2	3.4
DF-DF	1.7	9.7

analysis method (hereafter denoted "method I"). In Ref. 15 the method used was one sometimes employed in quasiclassical studies (hereafter denoted "method II"). In this method II, one calculates a quantity such as 8

$$\langle \Delta E_{\overline{\nu}} \rangle = (1/N) \sum_{i=1}^{n} \Delta E_{i}^{r} , \qquad (5.3)$$

where N is the total number of trajectories, the n indicates that one sums only the trajectories that have lost vibrational energy, and ΔE_i is the change in vibrational energy of the ith trajectory that has lost vibrational energy [the vibrational energy is calculated using Eqs. (5a)-(5g) of Ref. 39]. The probability for the internal state j-k transition (where j>k) is found by

$$P_{kl}(b, V_R) = \langle \Delta E_v \rangle (b, V_R) / (h \nu_{l-k})$$
 (5.4)

The cross section and rate constant are then calculated using Eqs. (4.7) and (4.8), respectively.

As a means of comparing method I with method II, in Table IV the V-V rate constants for the four systems discussed earlier in this section were calculated using both methods. (In each case the same trajectory data were used for the two methods.) It is quite evident from Table IV that use of method II yields a much larger V-V rate constant than does the cross-correlation method. Method II has previously been seen⁴⁷ to give substantially higher probabilities when compared with exact quantum mechanical results. A semiclassical justification has been given²⁷ only for method I: The moments used in our method I are analytic functions and are included in the class of operators whose expectation values have been equated quasiclassically and quantum mechanically via semiclassical arguments21 but the expectation value calculated for method II [Eq. (5.3)] is not based on an analytic function. The semiclassical arguments used to relate the quasiclassical and quantum mechanical moments cannot be applied to this operator or to method II.

In summary, in comparing Wilkins' ¹⁵ calculated rate constant of 9×10^{12} cc mol⁻¹ s⁻¹ there are two major differences compared with the present calculations, one of which (the potential energy surface) leads to reduced rate constants and the other (the method of calculating cross sections) which leads to enhanced values. The resulting agreement between the two calculations, due to cancelation, is thereby accidental.

VI. SUMMARY

In the present study of vibrational energy transfer, a quasiclassical cross-correlation has been used to relate

the correlation in changes in vibrational state of each molecule calculated via quasiclassical trajectories to probabilities and thereby to rate constants for V-V and V-R, T energy transfer.

Using the potential energy surface in Sec. II, ¹⁹ the V-V rate constant was calculated for Reaction (1.3), yielding a theoretical rate constant which agreed well with experiment with no adjustable parameters. Multiple collisions were found to contribute substantially to the V-V cross section. The V-R, T mechanism was found to be unimportant for this surface.

When a harmonic oscillator potential was used in place of the Morse potential in our study of Reaction (1.3), the rate constant was found to increase by a factor of 10. This increase is due to the fact that Reaction (1.3) is more nearly resonant for a harmonic oscillator potential than for the Morse potential case.

It was also found in this study that the calculated rate constant for Reaction (1.3) was about a factor of 4 smaller when using the Stockmayer potential of the Appendix, a potential which had (i) a shallower potential well and thereby fewer multiple collisions and (ii) had no vibrational coordinate short-range contribution.

The V-V rate constant calculated for the analogous DF reaction (5.2) was also in good agreement with experiment.

A comparison was made of calculated rate constants using the present cross-correlation method vs using one common (but not justified) quasiclassical one. The two methods showed a large disagreement, with the usual quasiclassical method consistently yielding rate constants from 2.5 to 17 times larger. This finding is in accord with the results of Muckerman et al. ⁴⁷ In Ref. 47, method II was found to give transition probabilities that were consistently too high when compared with numerically exact quantum mechanics.

ACKNOWLEDGMENTS ·

We are pleased to acknowledge the support of this research by the U. S. Department of Energy, the National Science Foundation, and by the University of Illinois Research Board through generous amounts of computer time. We also thank D. Secrest, E. Keren, W. K. Liu, and J. F. Bott for valuable discussions. This work is based on results of the Ph.D. thesis at the University of Illinois at Urbana-Champaign of one of us (M.E.C.). Portions of this work were performed while all three authors were at the University of Illinois, and support of this research there is gratefully acknowledged.

Contribution No. 6182 from the California Institute of Technology.

APPENDIX: STOCKMAYER INTERMOLECULAR POTENTIAL

We have performed one calculation of V-V energy transfer using a simpler potential energy surface suggested by Turfa *et al.* ³¹ but modified to include a dependence on vibrational coordinate. It is essentially a mod-

ified Stockmayer potential. 30 The usual Stockmayer potential is

$$4 \in [(\sigma/R)^{12} - (\sigma/R)^6] + \mu_1 \mu_2 (\cos \psi - 3 \cos \gamma_1 \cos \gamma_2)/R^3, \text{ (A1)}$$

where the angles are defined as follows: If R is a vector denoting the line joining the center of mass of the two molecules, and \mathbf{r}_1 and \mathbf{r}_2 denote their internuclear separation distances and orientations, respectively, the intermolecular angles γ_1 , γ_2 , and ψ are defined by

$$\hat{r}_1\cdot\hat{R}=\cos\gamma_1\;,\quad \hat{r}_2\cdot\hat{R}=\cos\gamma_2\;,\quad \hat{r}_1\cdot\hat{r}_2=\cos\Psi\;,\quad (A\,2)$$
 where \hat{r}_1 and \hat{R} denote unit vectors.

The functional form of the intermolecular potential used here has been given in Ref. 31, Eqs. (2.1)–(2.7). However, the potential of Ref. 31 is given with each molecule constrained to its equilibrium bond length. Thus, a Morse oscillator intramolecular vibrational potential has been added to the potential of Ref. 30. In addition, the dipole moment of each molecule has been made a function of its intramolecular bond length r as

$$\mu(r) = \mu_{eq} + (\partial \mu / \partial r)_{ren} \cdot (r - r_{eq}) , \qquad (A3)$$

where the subscript eq denotes values at the equilibrium bond length.

All of constants needed for this potential energy surface are readily obtainable from experimental measurements and are listed in Table V, with the exception of the Stockmayer parameters ϵ and σ . Stockmayer parameters can be determined from experimental studies of the temperature dependence of the molecule's bulk viscosity⁴⁸ and have been tabulated for many molecules. ^{30,48} However, such Stockmayer parameters are not found for HF. One cannot fit reasonable Stockmayer parameters to HF viscosity data⁴⁹ according to the prescription given in Ref. 48. The following alternate method to estimate ϵ and σ has been used.

As discussed by Turfa, 31 some workers 50-52 have taken

TABLE V. Parameters for the HF-HF Stock-mayer potential.

Parameter	Value	Footnote
r _{eq} (Å)	0.9171	а.
μ (D)	1.82	b
θμ/θ r (D/Å)	1.51	c
α" (cm³)	9.6×10 ⁻²⁵	d
α^{\perp} (cm ³)	7.2×10^{-25}	d
€/k (K)	74	е
σ (Å)	3.05	e

^aG. Herzberg, Spectra of Diatomic Molecules (Van Nostrand, New York, 1950), 2nd edition. ^bR. Weiss, Phys. Rev. 131, 659 (1963).

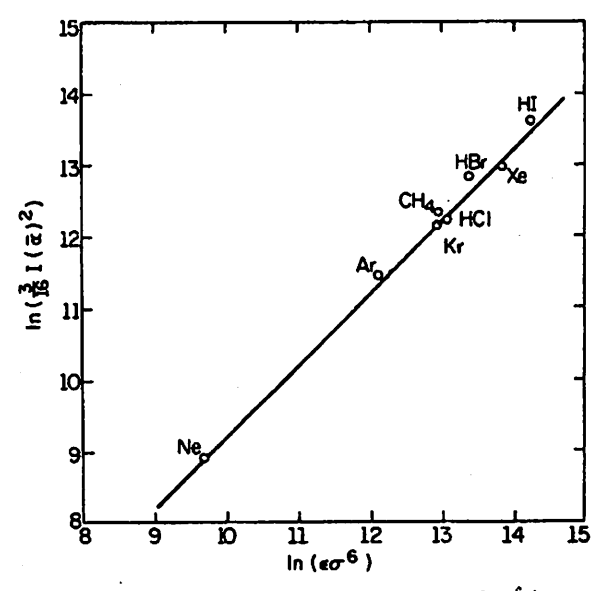


FIG. 5. Plot used to determine an estimate of $\epsilon \sigma^{\delta}$ for HF. Here *I* represents an ionization potential, and $\overline{\alpha}$ is the bulk polarizability.

the C' coefficient of the dispersion term in the potential Eq. (2,5) of Ref. 31 to be

$$C' = -\frac{3}{4}I_1I_2/(I_1 + I_2) , \qquad (A4)$$

where I_1 and I_2 are ionization potentials. The coefficient has also been taken to be³¹

$$C' = 2\epsilon \sigma^6 / (\overline{\alpha}_1 \overline{\alpha}_2) , \qquad (A5)$$

where α is a bulk polarizability. While these two coefficients are not equal, they are used to describe the same effect, and so are expected to be somewhat similar. Indeed, the plot of $\ln \epsilon \sigma^6$ vs $\ln [3I(\alpha)^2/16]$ shown in Fig. 5 for the other hydrogen halides and the rare gases that are isoelectronic with them is strikingly linear. Using the experimental value of $3I(\alpha)^2/16$ for HF and the data from the plot in Fig. 5, from a linear least-squares analysis we estimate that, for HF,

$$\epsilon \sigma^6 \approx 5.92 \times 10^4 \text{ K Å}^6$$
.

An independent estimate of either ϵ or σ to solve for the two unknowns is needed and was obtained as follows:

Dyke, Howard, and Klemperer⁵³ have determined the F-F distance in the HF-HF dimer to be 2. 79 ± 0.05 Å, with one HF bent $60^{\circ}-70^{\circ}$ from the F-F axis. The dimerization energy has been experimentally determined^{54,55} to be 6.0 ± 1.5 kcal mol⁻¹. Although the simple form that we are using for the potential cannot predict the nonlinear structure of the dimer, it does allow for an attractive well in the linear arrangement. We chose ϵ/k so as to yield the correct dimer F-F bond distance (2. 79 Å). For $\epsilon/k=74$ K and $\sigma=3.05$ Å, the resulting well depth of our potential was 3.91 kcal mol⁻¹. We have used these values for ϵ/k and σ in our calculation. However, this well depth is too small by 0. 6 to 3. 6 kcal mol⁻¹.

If one tried to adjust ϵ/k and σ so as to match the experimental well depth, the dimer F-F bond distance

^cR. E. Meridith, J. Quant. Spectrosc. Radiat. Transfer 12, 485 (1972).

^dH. Landolt and R. Bornstein, Zahlenwerte und Funktionen (Springer, Berlin, 1950), Vol. I, Chap. 3, p. 510.

This work.